

# Atomization of a G-DI spray with air dissolved in gasoline and mono-component fuels

L. Araneo<sup>\*1,2</sup>, R. Dondè<sup>2</sup>

<sup>1</sup>Politecnico di Milano, Energy Department, Milano, Italy

<sup>2</sup>CNR-ICMATE, Milano, Italy

\*Corresponding author: lucio.araneo@polimi.it

## Abstract

A spray from a GDI multi-hole injector is used to investigate and compare the atomization results from different fuels in which air has been dissolved to promote the atomization. The spray is injected in air at atmospheric conditions; three fuels are tested, a commercial gasoline with known distillation curves, and two mono-component fuels, n-hexane and n-heptane. The fuel is heated up to a constant temperature, between 30° and 120°C, and pressurised at 50 bars, a relatively low pressure used to improve the accuracy of the droplet sizing by PDA, thus allowing higher sensibility in detecting small variations of the measured quantity for better comparison among the results.

This work follows and completes a previous similar study on flash boiling, where no air had been dissolved into the fuels, and more fuels were tested. The global spray behaviours, like spray penetration and spreading angle, are illustrated by photographic results. Then the atomization is accurately measured by Phase Doppler Anemometry and results are analysed and compared. The spray droplet characteristics are measured at 45mm of axial distance from the injector tip in 13 different radial positions; after data post-processing the average velocity and diameters results are plotted, both as time evolution in a fixed position, and as radial profiles during the quasi-steady injection period.

When no air has been dissolved into the fuel, the temperature increase gives negligible effects up to the initial distillation or boiling point of each fuel, above which stronger variations are observed, with the typical spray collapse at increasing temperature.

When the fuel injected is saturated with air dissolved in it, the effects observed are very similar to those caused by flash boiling, but they start and become observable at temperature that are about 20 degrees lower. The major effects are the spray collapse, with a narrower shape, generally finer and more homogeneous atomization, and a remarkable lack of larger droplets, which results in a better atomization of the initial droplets of the spray

## Keywords

GDI Spray, fuel temperature, flash boiling, effervescent atomization, droplet sizing.

## Introduction

When a pure liquid is injected into an ambient to form a spray, flash boiling can occur if the vapour tension of the injected liquid is above the ambient pressure. In a similar way, if a gas is dissolved in the sprayed liquid, gas flashing happens if the fraction of dissolved gas is sufficiently above its limit of solubility in the liquid at its temperature and at the ambient pressure.

In a direct injection spark ignited engine, fuel flash boiling is often attained at low load due to the combination of the engine control strategy, the fuel is injected during the induction stroke, and of the evaporation characteristics of commercial gasoline, that starts at about 40°C. Fuel flash boiling could change the spray targeting [9], while the possible presence of gasses spontaneously dissolved in the fuel and of their effect is often not considered due to its negligible amount.

A previous study [7] was focused on the fuel flash boiling effects on droplet velocity and size properties at different temperatures, with the aim to highlight the conditions where the fuel composition can induce different behaviours that may be not negligible, and the final goal to scale the temperature effect on the different fuels.

The present study keeps the same set-up, methods, operative parameters and a reduced set of fuels of the previous study, and it is focused on the results measured when fuels with dissolved air are injected at different temperatures.

## Experimental Set-up

A standard production injector is used, the same sample tested in recent works [5] [6] [7]; it has a static flow rate of 13 mm<sup>3</sup>/ms (N-heptane at 100bar), used in GDI engines with relatively small cylinder capacity. It had been chosen because in its spray pattern, composed by five jets, one of the jet is well separated from the other four

and it is nearly axially oriented and thus easily accessible for optical techniques. **Figure 1** shows two views of the real spray at cold conditions, while **Figure 2** shows the nominal spray pattern at 45 millimetres from the injector tip, the injector reference coordinates ( $X_{INJ}$   $Y_{INJ}$ ), the position of the PDA system with its reference coordinates ( $X_{PDA}$   $Y_{PDA}$ ), and the accurate centring of the studied jet obtained by velocity measurements.

The spray is directed with the injector axis oriented vertically downwards, coincident with the PDA vertical axis ( $Z_{INJ}=Z_{PDA}$ ), and the electric connector direction identified as  $X_{INJ}$ . The injector is mounted in a rotating flange on the top of the closed bomb detailed in previous works [4], kept with open windows (100 mm diameter) and a slight air suction for continuous air renewal.

Spray images are visualized on a backlight telecentric photographic system, in fact a schlieren set-up used without the knife. A digital camera, a PCO Sensicam single shot fast shutter, is used to capture single images of the spray from front and side views, respectively the  $XZ_{INJ}$  and  $YZ_{INJ}$  planes. The image resolution is set at 10 pixel/mm, the exposure about 1 microsecond to use the whole dynamic range of the camera.

Droplet size is measured by a Dantec PDA configured to measure one velocity component, set vertically downstream directed as the injector axis  $Z$ , and the droplet diameter. The system includes an Ar+ laser operated at 512 nm, a fiber transmitting optic with a beam expander and a 310 millimeters focal length lens, a classic PDA receiver oriented at 70° side scattering with a 500 millimeters lens, a P80 processor, and its dedicated software. The measured velocity is set in the range -10 to 130 m/s, with the positive direction, coincident to the injection axis, directed downward in the laboratory; the droplet maximum diameter is limited at 80 microns.

Measurements are performed at  $Z = 45$  millimeters downstream of the injector tip, normally in 13 positions disposed along the axis parallel to  $X_{INJ}$  reported in red in the spray side view of **Figure 1b**, sometimes 16 positions are used at the highest temperature when the spray deviation is higher than usual. In the set-up preliminary tune-up, the axial velocity was measured also along the direction  $Y_{SPRAY}$ , to check that the studied jet was correctly centred and the symmetry was verified.

### Experimental Conditions

The fuel pressure is set at  $50\pm 0.5$  bar for more accurate PDA measurements, to avoid the common problems encountered at higher, although more engine-like pressures [1]. Thanks to the relatively low injection pressure, compared to a higher one, the fuel flow rate is reduced, the number of droplets produced is inferior and they show larger dimensions and lower velocity. Thanks to the large diameter, in the order of a tenth of micron, the relative measure accuracy is increased; it is also reduced the quantity of very small droplet, in the order of the micron, a dimension that is close to the light wavelength that limits the PDA inferior size range. The lower number of droplets decreases the probability of having two droplets at the same time in the measurement volume, thus reducing the probability of multiple signal that lead to lost measurements; and consequently reducing the bias of the PDA in favour of larger droplets.

The injector holder and the fuel line are heated up at the same temperature, set from 30 to 120 °C in steps of 10°C, sometime some value are skipped, depending on the studied parameter behaviour, to focus the study where the temperature variations has more evident effect on the studied parameters.

Double injections are used, with two logic pulses of 1 millisecond separated by a pause of 0.5 milliseconds. The results reported are relative to the second spray event, which has reached a more steady condition than the first one.

Five different fuels were available: two gasoline with sufficiently different distillation curves (same batches used in [6][7]), and three pure components; the distillation curves are reported in **Figure 2**. In this work n-Heptane and Hexane are mostly used, since mono-component fuels have a defined saturation curve, which allows to define easily a reference temperature for comparison and rescaling. Also the gasoline Fuel06 is used but for a limited set of test, since it had already been demonstrated that the observed phenomena are similar in mono- and multi-component fuels, and scale quite well with their superheat degree [12] [13] [14]. However in multi component fuels other parameters like the bubble pressure [1] [3] [6] [14] or the Jacob number [6] [14] may be difficult to define or calculate.

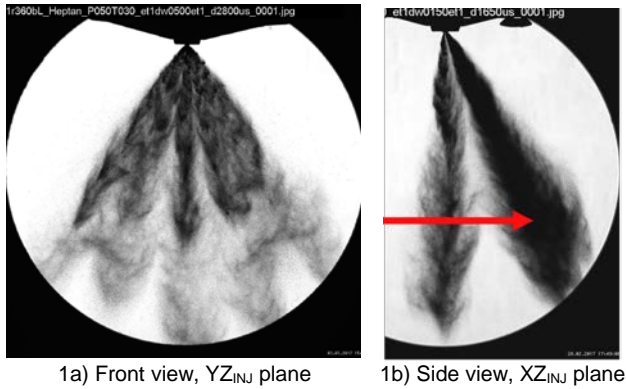


**Figure 1.** Front and. side view of the spray, in red the axis for the PDA measurement (parallel to  $X_{INJ}$ , at  $Y_{INJ}=0$ ,  $Z=45\text{mm}$ )

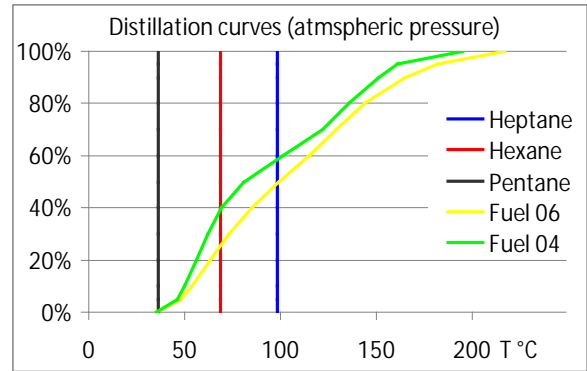


**Figure 2.** The distillation curves of the fuels used

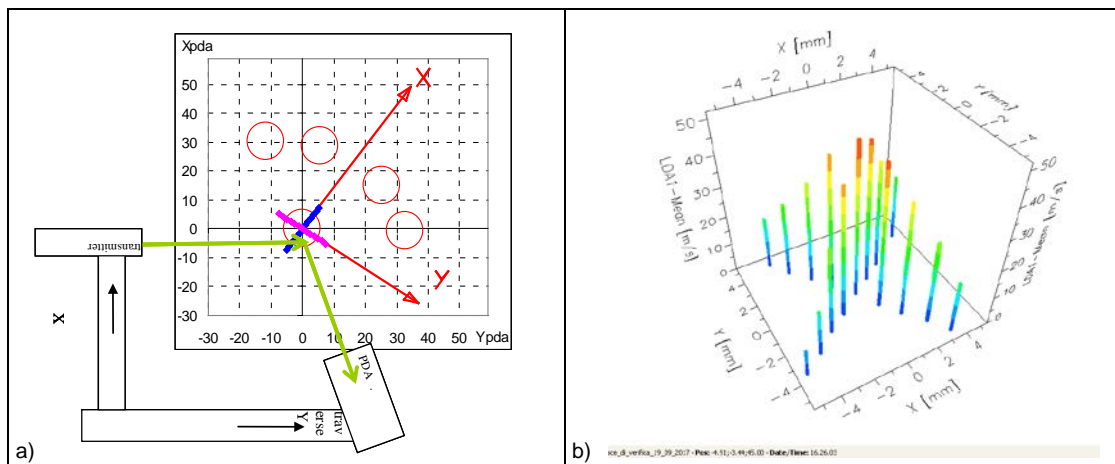


**Figure 3. a)** The spray nominal pattern at  $Z=45\text{mm}$  with its reference system  $XY_{\text{Spray}}$  in red. The PDA optic system is indicated (not in scale) with the laser path in green and its reference system  $(X_{\text{PDA}}, Y_{\text{PDA}})$  centred on the studied jet. **b)** Centering of the studied jet at cold conditions (quasi-steady average axial downstream velocities,  $XY_{\text{PDA}}$  coordinates).

The air used to pressurised the fuel is at the same time dissolved in it at 50 bar. The air inlet is located along the short connector between the injector and the pressurised fuel reservoir. As long as fuel is consumed, new air is pumped in the reservoir; the air bubbles rise from its bottom and keep the liquid mixed and saturated by the air, which accumulated on the top of the reservoir. The amount of air dissolved in the fuel was estimated by measuring the relative volumes of the two fluids after release and separation in a transparent tube at ambient conditions. The values measured ranged between 10 for heptane and 14 for hexane (equivalent to a mass ratio about 1.5% and 2.2% respectively), in acceptable accordance with few data found in the literature [9], that would give about 12 for heptane and 14 for hexane.

The time evolution of the spray shape from its side view at cold conditions (Fuel06 at  $30^\circ\text{C}$ ) is given in **Figure 4**; the spray timing compared to the logic pulse is influenced by the different opening and closing mechanical delays, and the closing phase is not as sharp as the opening one. The first injection lasts from 0.3 to 1.4 ms, then after the pause of about half millisecond, the second spray is injected. Note that when the injector closes, the vertical jet is suddenly attracted (**Figure 4**, delays 1.5 and 1.9 ms) to the right side by the other four jets, whose momentum and consequently air entrainment are much stronger than those of the studied single jet.

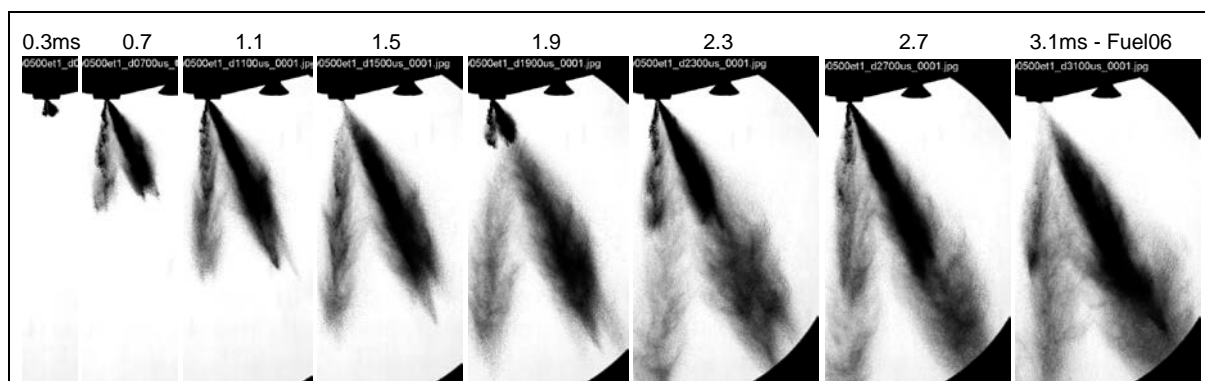


Figure 4. Time evolution of the double injection event. Fuel 06,  $T=30^{\circ}\text{C}$

Figure 5 shows the fuel temperature effect at a fixed delay ( $t=2.7$  ms) on the same Fuel06, with the fuel temperature kept constant from  $30^{\circ}\text{C}$  up to  $120^{\circ}\text{C}$ , when the vertical jet is nearly disappearing because merging with the other jets. This temperature is also the maximum mechanically possible for the injector.

Figure 5 shows similar photos for Fuel06+air, whose test temperature is limited up to  $80^{\circ}\text{C}$ , beyond which the vertical jet can not be distinguished any more.

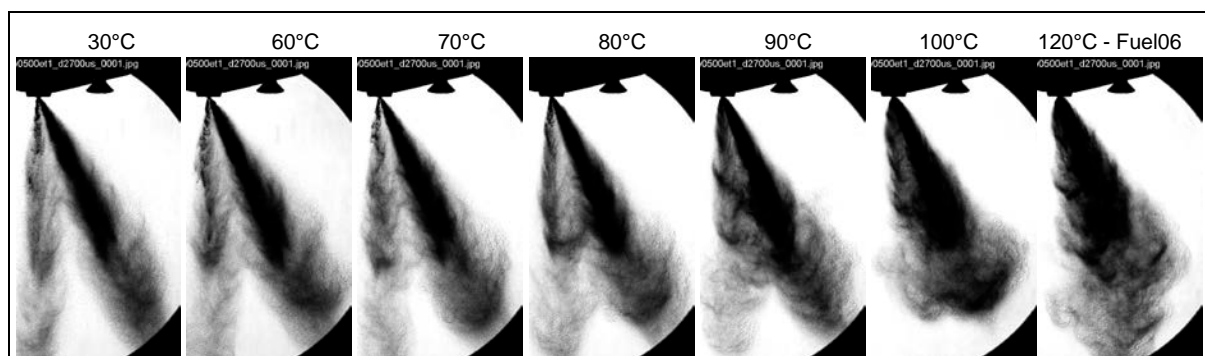


Figure 5. Fuel06 Spray: temperature effect at fixed delay 2.7 ms.

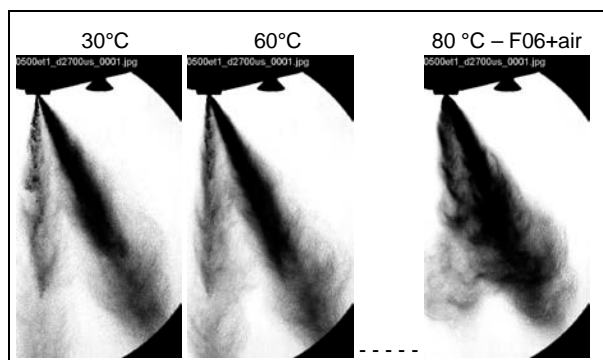
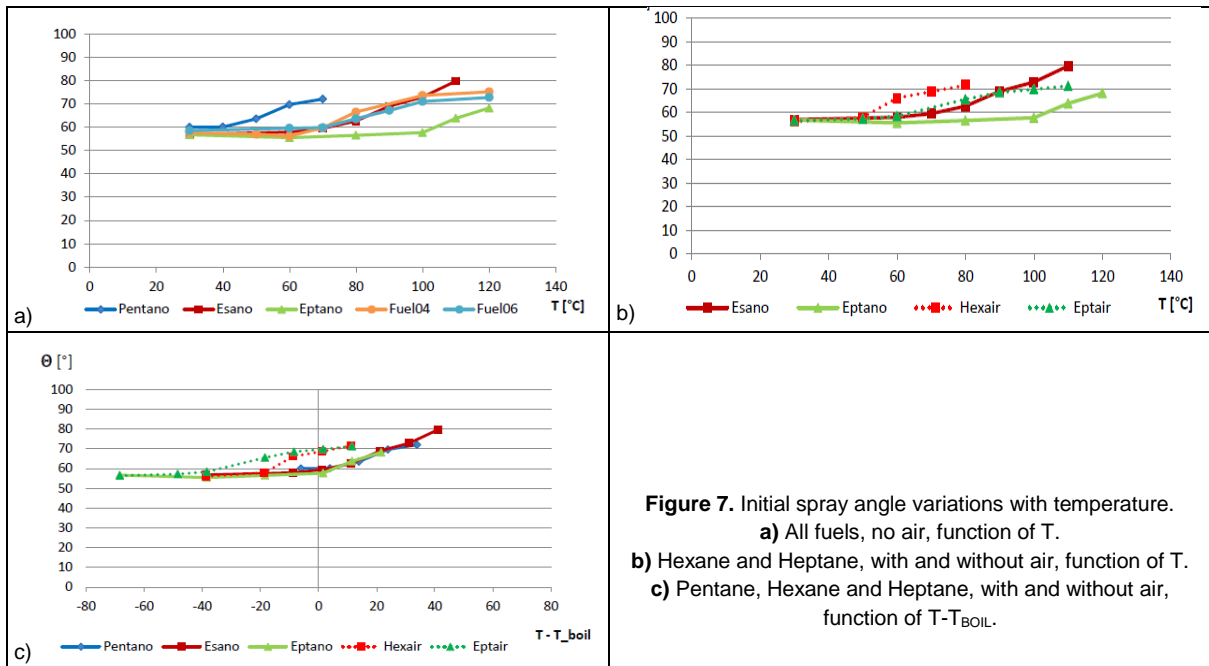


Figure 6. Fuel06+air: temperature effect at fixed delay 2.7 ms

### Image acquisition and processing

For each test condition, a set of images is acquired to observe the spray evolution. Starting from the injection trigger signal, images are acquired every  $100\mu\text{s}$  up to  $3.5$  ms, when the event is nearly ended. For each delay, 10 images are acquired for statistical analysis. The image taken at delay=0, yet with no spray, is used as background for image processing; when subtracted, the possible shot-to-shot flash intensity variation is also corrected for. From each image, the spray length and width at various positions are extracted and used to calculate some typical parameters, among which the initial spray angle, measured in the first millimetre close to the nozzle where it shows high sensitivity to gas or vapour flashing. The results are reported in Figure 7 as a function of the fuel temperature, for different test conditions. In Figure 7a. The value is reported for the five tested fuels with no air added. It is evident how the spray angle increases when the temperature passes each fuel boiling point, and that two real gasolines are very similar among them, and much more similar to the N-hexane than to the N-heptane. Figure 7b reports the spray angle comparison for Heptane and hexane with and without air; the effect of the air in

the spray angle is visible starting from 20 to 30 °C before its boiling point. Figure 7c puts together the result for pure fluids, rescaled as a function of the temperature difference from boiling point  $T-T_{boil}$ .



**Figure 7.** Initial spray angle variations with temperature.

a) All fuels, no air, function of T.

b) Hexane and Heptane, with and without air, function of T.

c) Pentane, Hexane and Heptane, with and without air, function of  $T-T_{BOIL}$ .

### PDA data acquisition and processing

At each measurement position injections are operated at 5 Hz for 100 seconds, to collect up to 200'000 droplets.. Averages are calculated over time bins 0.1 ms long; the PDA bias towards larger diameter is also evaluated and corrected. A synthetic example of the results is reported in Figure 8, where per each time bin are reported the droplet average velocity and diameters  $D_{10}$ ,  $D_{20}$ ,  $D_{30}$ ,  $D_{32}$  calculated over the 500 injections. The logical injection pulse is reported in the lower part of the graph; the delay of the first measured data is partially due to the sum of to the mechanical injector delay and to the convection time up to the measurement position that is 45 mm downstream.

At each conditions, the result reported are those obtained in the measured plume, identified as the position where the largest velocities are measured during the time window from 2.8 to 3.3 milliseconds, corresponding to the second injection. Due to the spray collapse at higher temperature, the measured spray plume shifts towards the photo right side, that is to largest  $X_{INJ}$ . The velocity spatial profile is shown in the next paragraph.

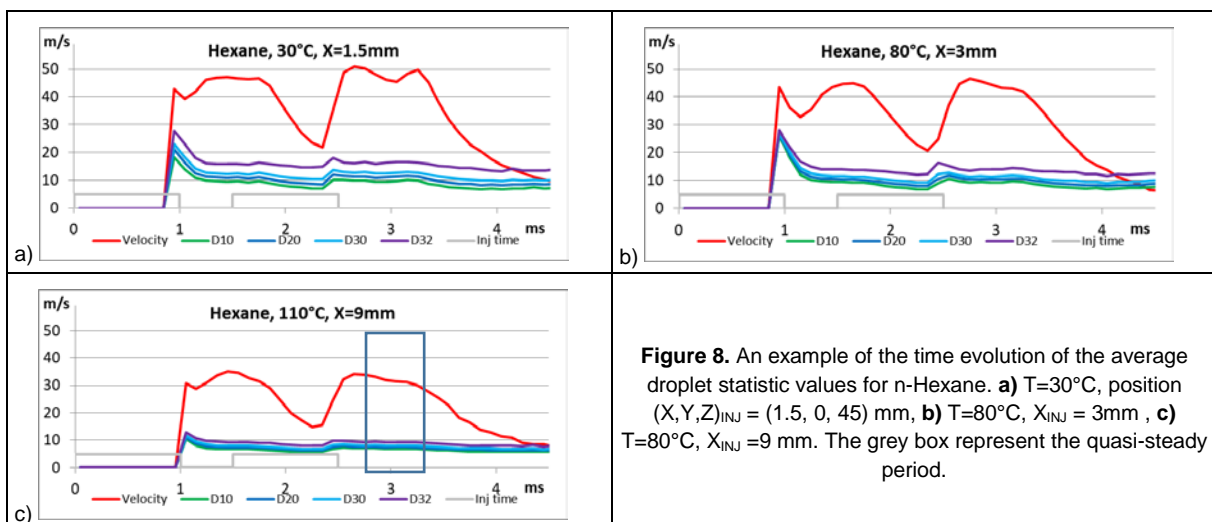


**Figure 8.** An example of the time evolution of the average droplet statistic values for n-Hexane. a)  $T=30^{\circ}\text{C}$ , position  $(X,Y,Z)_{INJ} = (1.5, 0, 45)$  mm, b)  $T=80^{\circ}\text{C}$ ,  $X_{INJ} = 3$  mm, c)  $T=110^{\circ}\text{C}$ ,  $X_{INJ} = 9$  mm. The grey box represent the quasi-steady period.



### Further results and discussion

The data of Figure 8 shows some typical behaviours of GDI sprays. The first pulse at cold conditions shows the initial burst of fast and big droplets, that is most probably an issue of an aero-dynamical selection, where the large droplets produced by the poor atomization of the pre-jet are not efficiently slowed down by the air drag. Note that their number is very limited, few droplets over 500 positions, while in the following time bins thousands of droplets are measured. This burst of large droplets is much less visible at the second pulse, probably because of the presence of the smaller droplets that reduced their statistical influence, as already speculated in a previous work [8] with wider analysis of double injections. As already suggested, this burst may be reduced by different mechanisms: better atomization, faster evaporation, and a data processing effect due to time windowing

From the data used to build Figure 8, it is calculated also the quasi steady velocity value during the second pulse, by averaging the droplet velocities in a unique longer time window from 2.8 to 3.3 ms. The same values are calculated from each tested position, thus the spatial profile of the quasi steady period is built, for each fuel at each temperature; the results are reported in Figure 9.

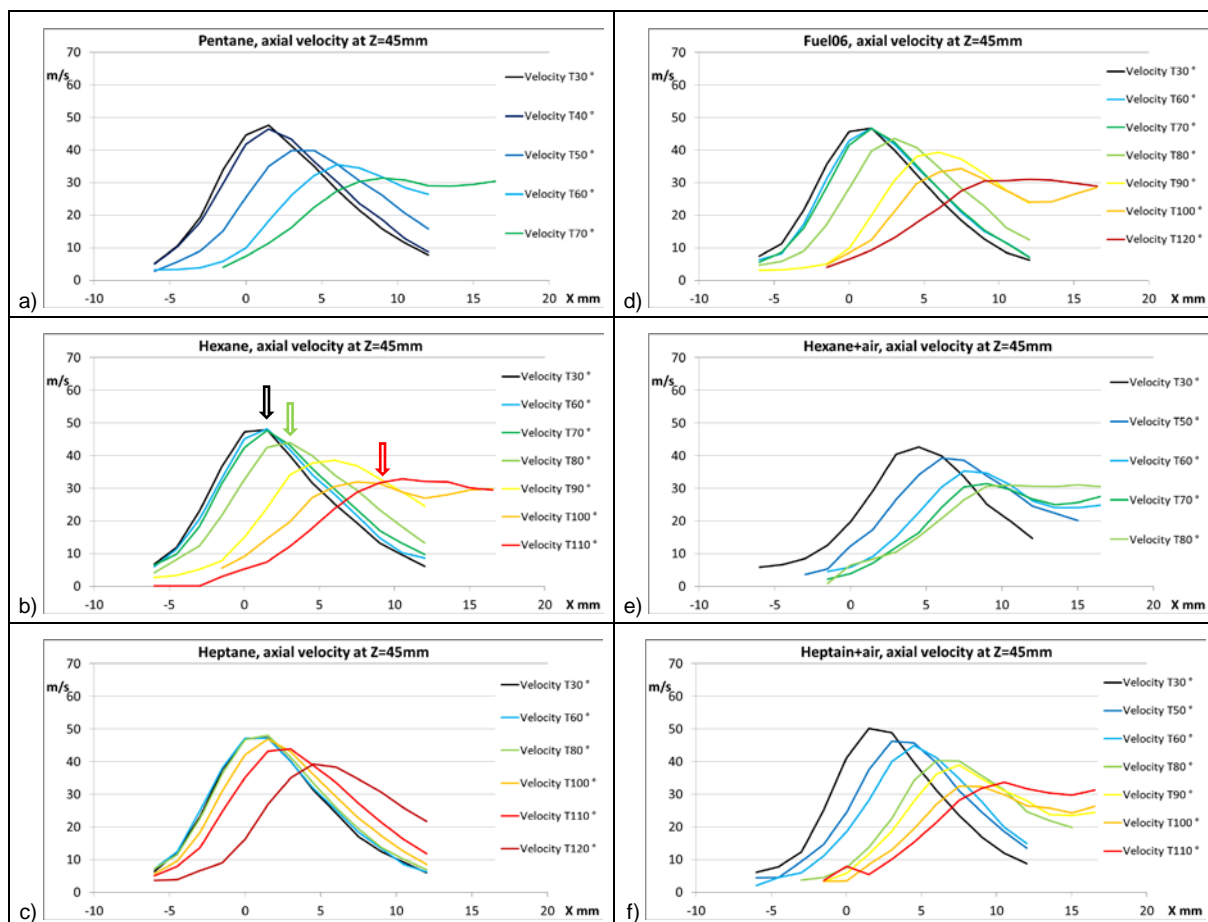


**Figure 9.** Spatial profiles, along  $X_{INJ}$  ( $Y=0, Z=45\text{mm}$ ), of the quasi steady droplet average velocity (time window 2.8-3.3ms) for four fuels, and two pure fluid with air dissolved, at different temperatures (few value were not tested, colour coding is kept). In b) the arrows indicates the points obtained from the previous Figure 8.

The spray profile shifts towards the right side at higher temperature is clearly visible when the fuel temperature is about a tenth of degrees Celsius above the pure components boiling point: at  $50^\circ\text{C}$  for the pentane ( $T_{\text{boil}} = 36^\circ\text{C}$ ), at  $80^\circ\text{C}$  for N-hexane ( $T_{\text{boil}} = 69^\circ\text{C}$ ), at  $110^\circ\text{C}$  for N-heptane ( $T_{\text{boil}} = 98^\circ\text{C}$ ). For the gasoline Fuel06 it is clearly visible at  $80^\circ\text{C}$ .

At higher temperature the velocity profile is extended to the right side where the increase of the other jets become visible; at very high temperatures, the jets fully merge and the velocity profile shows a wide flat plateau.

From the data of Figure 9, the maximum values of the velocity profiles are plotted against the corresponding temperature and reported in Figure 10. For all the fuels the velocity is almost constant up to its boiling temperature, beyond which a sharp decrease is measured. Note that the segments between two measured point should be intended only as a graphical aid for better visualization purpose, they do not represent a correct result trends between real data.

The data of Figure 10 belonging to the pure components are also plotted against the overheat degree ( $T - T_{\text{BOILING}}$ ) in Figure 11; the data from gasoline could not be elaborated since its boiling temperature is not defined. In this last plot it is clearly evident that the velocity data are very well scaled by the superheat degree.

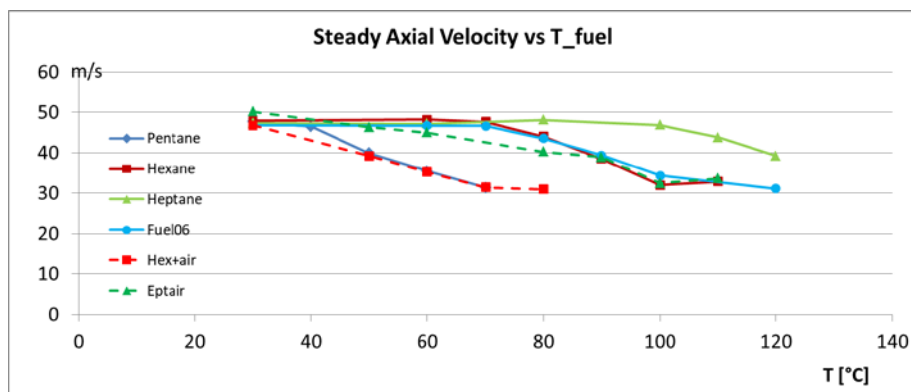


**Figure 10.** Maximum value of the quasi steady droplet average velocity (spatial profiles along X, time window 2.8-3.3ms) for the tested fuels, at different temperatures

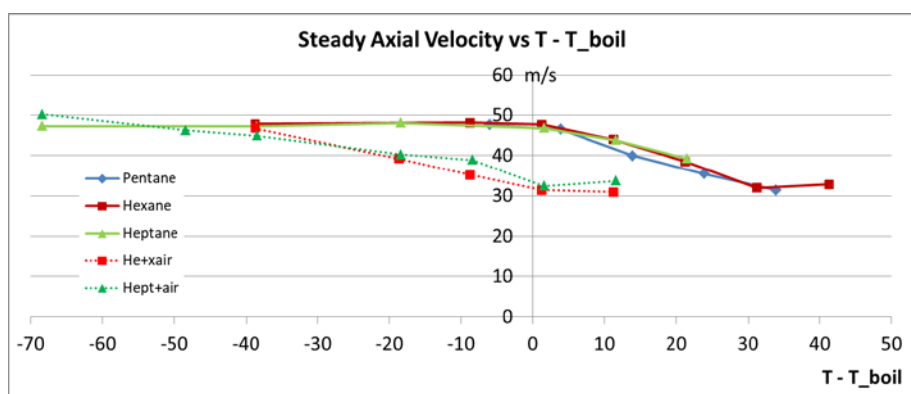


**Figure 11.** The same data of Figure 10 reported as a function of  $T - T_{\text{boiling}}$ , for the three pure components.

## Conclusions

A GDI spray was successfully used to compare the behaviors of different fuels, a gasolines and three mono-component hydrocarbons, also with dissolved air, at temperatures between 30°C and 120°C, a range where flash boiling is expected to induce a strong change in the spray shape. The images and the droplet velocity measured by PDA are used to calculate the overall spray velocity profiles, that are used as indicators for the comparison. The effect of dissolved air is to anticipate the effect normally due to the phenomena of flash boiling.

## Acknowledgements

The authors acknowledge Mr. Sergio Cerutti from Politecnico di Milano for his contribution to the work as part of his Engineering Master Thesis.

## References

- [1] Aleiferis, P. G., Van Romunde, Z., R., Fuel 105: 143-168 (2013).
- [2] Araneo, L., 2012, 12th Triennial International Conference on Liquid Atomization and Spray Systems, Heidelberg, Germany, September 2-6, 2012, ISBN 978-88-903712-1-9.
- [3] Araneo, L., Ben Slima, K. and Dondé, R., Sept 5-7, 2002, 18th European Conference on Liquid Atomization and Spray Systems
- [4] Araneo, L., Coghe, A., Brunello, G., Dondé, R., SAE Paper 2000-01-1901.
- [5] Araneo L., Dondé R., Sept 4-7, 2016, 27th Annual Conference on Liquid Atomization and Spray Systems,
- [6] Araneo L., Dondé, R., 2017, Fuel 191: pp.500–510.
- [7] Araneo L., Dondé, R., July 2018 Triennial International Conference on Liquid Atomization and Spray Systems
- [8] Araneo L., Dondé R., Postriotti, L., Cavicchi, A., September 2017, 28th Annual Conference on Liquid Atomization and Spray Systems. ISBN 9788490485804.
- [9] Battino, R.; Tominaga, T., 1984 Journal of Physical and Chemical Reference Data

- [10] Khan, M. M., Helie, J., Gorokhovski, M. and Nadeem, S., 2017 Applied Thermal Engineering, 123: pp377-389, 10.1016/j.applthermaleng.2017.05.102.
- [11] Kumagai, S., 1957, 6th International Symposium on Combustion, Vol 6, pp.668-674 10.1016/S0082-0784(57)80093-9.
- [12] Mojtabi M., Chadwick N., Wigley G., Helie J., Sep. 8-10, 2008, 22nd European Conference on Liquid Atomization and Spray Systems
- [13] Yanfei L, Hengjie G, Xiao M, Yuliang Q, Zhi W, Hongming X, Shijin S, 2017, Fuel 211: pp.38–47, 10.1016/j.fuel.2017.08.082
- [14] Zeng, W., Xu, M., Zhang, G., Zhang, Y., Cleary, D. J., 2012Fuel 95: pp.287-297